

Efficient sensitization of mesoporous TiO₂ film with CdSe nanospherical particles for application in dye-sensitized solar cell

BENYAMIN YARMAND

Nanotechnology and Advance Materials Department, Materials and Energy Research Center, Karaj, Iran

Dye-sensitized solar cells were successfully fabricated from sensitized mesoporous TiO₂ films which consist of CdSe nanospherical particles. Sensitization was carried out by successive ionic layer adsorption and reaction (SILAR) process through five cycles. Scanning electron microscope (SEM) images confirmed the formation of CdSe individual nanospherical particles on the surface of mesoporous TiO₂ films. With the enhancement of SILAR cycles, the number of CdSe nanospherical particles were increased so much that after five cycles, they joined and formed a porous cover on the surface of mesoporous TiO₂ film. The absorbance spectra measured by UV-Vis spectrophotometer revealed that with the enhancement of SILAR cycles, the absorption of the films increased and the absorption edges shifted to the longer wavelengths. Photovoltaic measurements clarified that the short circuit current and the open circuit voltage were increased with the enhancement of SILAR cycles and reached to 6.59 mA/cm² and 0.742 V after five SILAR cycles, respectively. As a result, the maximum power conversion efficiency of 2.93 % was obtained after sensitization of five SILAR cycles.

(Received June 23, 2014; accepted January 21, 2015)

Keywords: Dye-sensitized solar cell, CdSe nanospherical particles, Mesoporous TiO₂ film; SILAR process

1. Introduction

Since the invention of dye-sensitized solar cells (DSSCs), numerous and extensive researches have been carried out to improve photovoltaic performance and commercialize it so far. This is because these cells have the potentiality of replacing the conventional silicon-based solar cells due to their low cost and little environmental damaging impacts [1, 2].

Using TiO₂ films with their mesoporous structure in the photoanode of DSSCs can have a very good effect on the cell performance because of the suitable position of the TiO₂ band energy and the high photoelectric response, and when these films are formed with mesoporous structure, their efficiency is multiplied because of the enhancement of the specific surface area, the preparation of continuous pathways for the electron movements in the structure, and also a better diffusion of electrolyte carriers. In spite of this, the power conversion efficiency of these cells is still low as they have poor ability for light harvesting and electron recombination during the charge transport [3-6].

Currently, one of the best ways to improve the cell performance is to use chalcogenide semiconductor nanoparticles as a photosensitizer on mesoporous TiO₂ films. The energy gap of semiconductor nanoparticles can be tuned by controlling their sizes; as a result of this, the absorption spectrum can be adjusted to match the spectral distribution of the sun. Semiconductor nanoparticles have large extinction coefficients due to the quantum confinement effects. Moreover, these nanoparticles have

large intrinsic dipole moments, which may lead to a rapid charge separation [7-10]. Among different semiconductors, such as CdTe, CdS, and etc, CdSe shows a more effective performance as a photosensitizer since it has got a suitable band gap, long life, excellent stability, and easy fabrication [11,12]. The main problem regarding the sensitization of mesoporous TiO₂ films with semiconductor nanoparticles like CdSe is the way they are assembled on the film because in an inappropriate deposition condition, nanoparticles may sediment and block the entrance of the pores and consequently prevent from the diffusion of electrolyte carriers, which results in a poor cell performance [13,14].

Among all the existing alternatives, the best way for in situ formation of CdSe nanoparticles on mesoporous TiO₂ films is the simple and low cost process of successive ionic layer adsorption and reaction (SILAR) which enables a precise control over the nucleation and growth of nanoparticles. SILAR method involves the adsorption of a Cd²⁺ precursor on the TiO₂ surface and subsequently, its reaction with a Se²⁻ precursor, which leads to the formation of CdSe on TiO₂ surface [15, 16].

In the present research, with the aim of increasing the power conversion efficiency, DSSCs based on mesoporous TiO₂ films have been sensitized by CdSe nanoparticles, and for a more effective sensitization and prevention from the pores of TiO₂ films being blocked, these nanoparticles have been formed individually with a novel nanospherical shape by SILAR process and their performance has been investigated and discussed.

2. Experimental

2.1. Preparation of mesoporous TiO₂ photoanode

Mesoporous TiO₂ photoanodes were prepared by sol-gel templating technique. 5 g of titanium tetraisopropoxide (Merck) was hydrolyzed using 3.2 g of hydrochloric acid (Merck) under stirring for 10 min. The hydrolyzed sol was mixed with 1 g of Pluronic P123 (Aldrich) surfactant dissolved in 21 g of ethanol (Merck). Subsequently, FTO substrates with sheet resistance of 10 Ω/□ (Solaronix) were coated with spin coater at 2000 rpm for 30 s. The films were then aged at 10 °C for 24 h under controlled humidity of 65-75 %. The samples were finally annealed in a tube furnace at 400 °C for 1 h under air with a heating rate of 1 °C/min. The films were thickened about 1 μm after ten deposition cycles.

2.2. Sensitization of photoanode

Photoanodes were initially in situ sensitized by CdSe nanospherical particles grown by SILAR processes. Photoanodes were successively immersed in two different solutions for 5 min each, first in aqueous solution containing 0.5 M Cd(NO₃)₂ and then in Na₂SeSO₃ aqueous solution at 50 °C. The Na₂SeSO₃ aqueous solution was prepared by refluxing 0.3 M Se (Merck) in an aqueous solution of 0.6 M Na₂SO₃ (Merck) at 70 °C for 6 h. Following each immersion, the photoanodes were rinsed with water, and then were dried, respectively. All these processes are termed as one SILAR cycle and repeated five cycles. After that, photoanodes were immersed in 0.5 mM ethanolic solution of *cis*-diisothiocyanato-bis(2,2′-bipyridyl-4,4′-dicarboxylato) ruthenium(II) bis(tetrabutylammonium) (N719, Solaronix) and kept at room temperature for 72 h. The dye-adsorbed photoanode was then rinsed thoroughly with ethanol and subsequently dried.

2.3. Preparation of counter electrode

Pt catalysts as the counter electrode were prepared by spreading a drop of 10 mM H₂PtCl₆ (Merck) in isopropanol (Merck) on FTO substrate and heating it to 400 °C for 15 min under air ambient.

2.4. Preparation of electrolyte

The polysulfide electrolyte prepared freshly by dissolving 0.5 M Na₂S (Merck), 0.2 M S (Merck), and 0.2 M KCl (Merck) in ultrapure water/methanol (7:3 by volume).

2.5. DSSC assemblage

The sensitized photoanode and counter electrode were assembled into a sandwich type cell and sealed by 25 μm thick thermoplast hot-melting sealing foil (SX 1170-25, Solaronix). The electrolyte was injected into the cell by capillary forces through a hole drilled in the counter electrode. The hole was covered and sealed with a quickly solidifying epoxy polymer to prevent fluid-type electrolyte leakage. The cells had an active area of 0.25 cm².

2.6. Characterization and measurements

The morphology of the films and prepared nanoparticles was observed using transmission electron microscope (TEM, CM200 FEG, Philips) and scanning electron microscope (SEM, 360, Cambridge), respectively. The surface relief of the films was studied using atomic force microscope (AFM, CP, Auto probe). The optical absorbance spectra of the films were recorded using a UV-Vis spectrophotometer (Lambda 25, Perkin Elmer) with a scanning rate of 60 nm/min in the wavelength range of 300 – 800 nm. Photovoltaic measurements were performed under 1 sun AM 1.5G simulated sun light using a solar simulator (luzchem) and a potentiostat/galvanostae (PGSTAT 302N, Autolab, Eco-Chemie).

3. Results and discussion

3.1. TEM analysis

The mesoporous structure of TiO₂ film that used as photoanode was investigated by TEM microscope. Fig. 1 shows TEM image of the mesoporous TiO₂ film. It could be observed that anatase nanocrystals connect with each other to produce a framework consisting of mesopores. Furthermore, the inset exhibits the corresponding selected area electron diffraction (SAED) patterns that include rings with spots confirming the presence of very small anatase nanocrystallites. The estimated size of anatase nanocrystals are about 5 nm.

3.2. Microstructure

Fig. 2 illustrates the surface of the CdSe nanospherical particles sensitized mesoporous TiO₂ films after different SILAR cycles. In Fig. 2a, it could be seen that after one SILAR cycle, a very small number of CdSe individual nanoparticles with spherical shape have been formed on mesoporous TiO₂ film. In Fig. 2b, it is illustrated that after two SILAR cycles, more CdSe nanospherical particles have been formed on mesoporous TiO₂ film. The size

range of these nanospherical particles is wider than the previous cycle which is due to the better growth of the formed nanospherical particles in the first SILAR cycle compared with the second SILAR cycle. This is because the surface of the formed particles in the initial cycles is a preferred site for adsorption of ions and their reaction in the following cycles. As it could be observed in Fig. 2c-e, with the enhancement of SILAR cycles, the number of the CdSe nanospherical particles formed on mesoporous TiO₂ films has been increased so much that after five SILAR cycles, the CdSe nanospherical particles are joined together and have created a continuous porous cover on the mesoporous TiO₂ film.

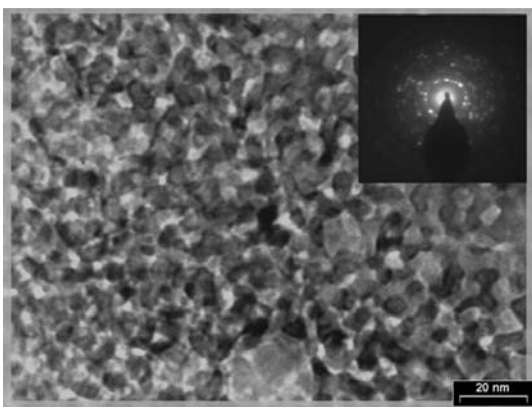


Fig. 1. TEM image of the mesoporous TiO₂ film, the inset is a selected area electron diffraction of the sample.

3.3. AFM analysis

Fig. 3 shows AFM's 3D topographies of the surface of the CdSe nanospherical particles sensitized mesoporous TiO₂ films after different SILAR cycles. As it could be seen, all the samples present approximately a uniform hill-valley like morphology. The root mean square (RMS) roughness after one SILAR cycle is 3.005 nm. With the enhancement of the SILAR cycles, the RMS roughness is increased so much that reaches to 21.660 nm after four SILAR cycles, but it falls to 7.361 nm after five SILAR cycles. The increase of RMS roughness after one to four SILAR cycles is owing to the rise in the number of the formed CdSe nanospherical particles on the surface of the mesoporous TiO₂ films and also their sizes being increased which is demonstrated in the figures. However, after five SILAR cycles the RMS roughness is decreased in spite of the CdSe nanospherical particles being bigger than the previous cycles and this is due to their attachment which forms a uniform cover which reduces the distance between the hill and the valley.

3.4. Optical characterization

Using the absorbance of UV-Vis spectrum, the incorporated amount of CdSe nanospherical particles on mesoporous TiO₂ films was evaluated. The absorbance spectra of the CdSe nanospherical particles sensitized mesoporous TiO₂ films after different SILAR cycles are shown in Fig. 4a. All the films exhibit low absorption in the visible region which is enhanced with their entrance to the ultraviolet region. It could be observed that after one and two SILAR cycles, the absorption in the longer wavelengths which are more than 500 nm is almost the same whereas in the shorter wavelengths, the absorption increases as the number of SILAR cycles increases. By increasing SILAR cycles, absorption of films has a gradual but considerable enhancement in the ultraviolet and visible regions, and the absorption edges are shifted to the longer wavelengths which are known as red-shift. Absorption enhancement of the films is due to the rise in the number of the formed CdSe nanospherical particles on the surface of the mesoporous TiO₂ films which are seen in the SEM images and the red-shift of the absorption edges are because of the growth of CdSe nanospherical particles [11, 14]. As a result, CdSe nanospherical particles could be considered as the secondary particles which have been formed by the aggregation of smaller quantum dots [12].

Fig. 4b illustrates the difference of the absorbance of mesoporous TiO₂ films without and with CdSe sensitization after different SILAR cycles. The effect that the sensitization of CdSe nanospherical particles leaves on the mesoporous TiO₂ films could be easily noticed due to the difference of absorbance spectrum when a board absorbance peak has been observed in ultraviolet and visible regions. This indicates that the CdSe nanospherical particles are more photoactive and mainly responsible for the electron generation in these regions. The difference of absorbance spectrum of CdSe nanospherical particles which is prepared after five SILAR cycles shows a higher value than the samples of CdSe nanospherical particles which are prepared in the other SILAR cycles.

3.5. Photovoltaic performance of DSSCs

The photocurrent density-voltage (J-V) characteristics of the DSSCs made of CdSe nanospherical particles sensitized mesoporous TiO₂ films after different SILAR cycles are shown in Fig. 5. In addition, the corresponding photovoltaic parameters, such as short circuit current (J_{sc}), open circuit voltage (V_{oc}), fill factor (FF) and power conversion efficiency (η) are all summarized in Table 1.

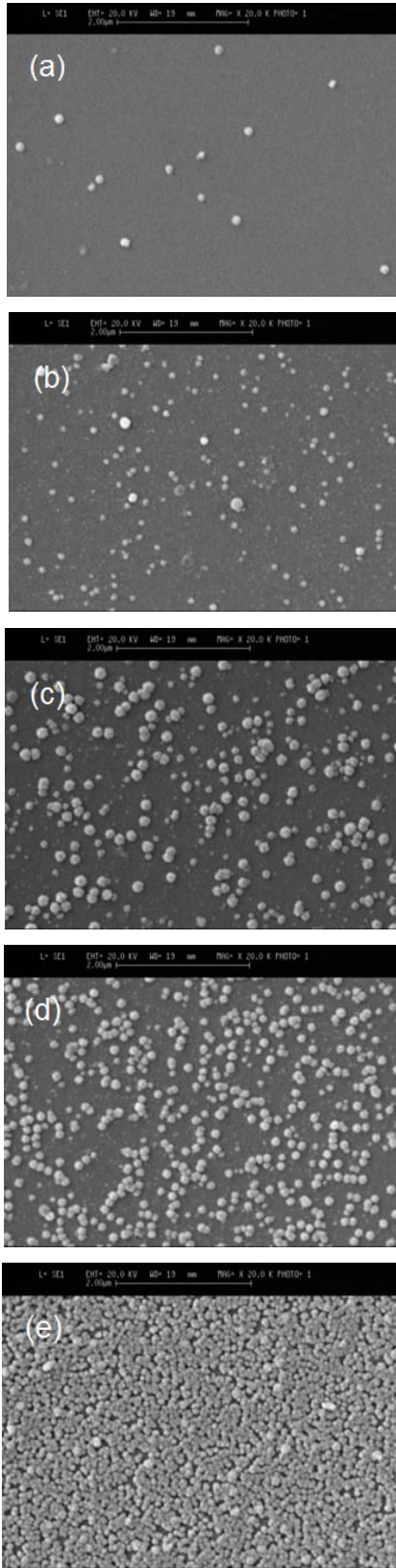


Fig. 2. SEM images of the CdSe nanospherical particles sensitized mesoporous TiO₂ films after (a) one, (b) two, (c) three, (d) four and (e) five SILAR cycles.

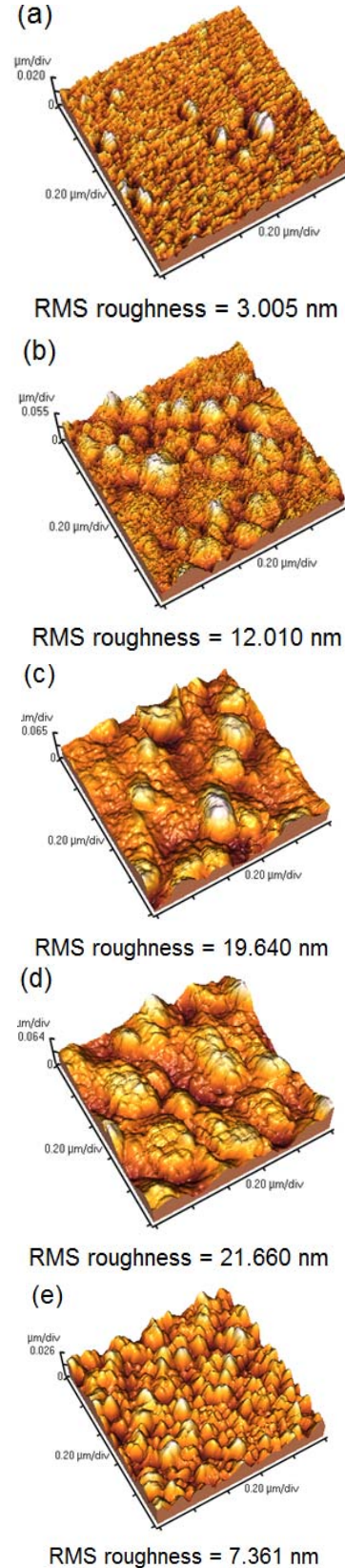


Fig. 3. AFM images of the CdSe nanospherical particles sensitized mesoporous TiO₂ films after (a) one, (b) two, (c) three, (d) four and (e) five SILAR cycles.

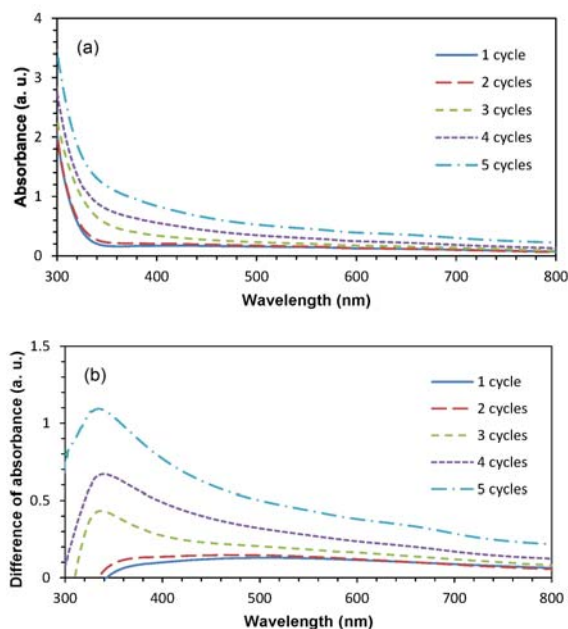


Fig. 4. (a) Absorbance spectra of the CdSe nanospherical particles sensitized mesoporous TiO₂ films, and (b) difference of absorbance of mesoporous TiO₂ films without and with CdSe sensitization after different SILAR cycles.

It could be observed that as the SILAR cycles proceed from one to five, the short circuit current from 5.40 to 6.59 mA/cm² and open circuit voltage from 0.721 to 0.742 V have increased. As a consequence of these changes, the solar cell sensitized by CdSe nanospherical particles has the minimum power conversion efficiency of 2.22 % after one SILAR cycle and reaches to the maximum power conversion efficiency of 2.93 % after five SILAR cycles. The enhancement of the short circuit current is resulted from a rise in the number of formed CdSe nanospherical particles on the surface of mesoporous TiO₂ films. As a result of this enhancement, these particles absorb a bigger share of incident light and consequently, more electrons are injected to TiO₂'s conduction band which causes an increase in charge injection efficiency. After one and two SILAR cycles, short circuit current enhances slightly since the number of formed CdSe nanospherical particles on the surface of mesoporous TiO₂ films is small; however, after three and four SILAR cycles, this enhancement is greater. After five SILAR cycles, due to the large number of CdSe nanospherical particles, some of the pores of the mesoporous TiO₂ film are blocked which lead to a decrease in the regeneration rate owing to the lack of diffusion of electrolyte carriers and also the cell efficiency enhances less considerably. As a result, it is expected that the cell efficiency do not enhance due to the pores of mesoporous TiO₂ film being blocked as the number of SILAR cycles goes up [12, 17]. The enhancement of open circuit voltage is because of the decrease in the recombination rate of electrons with electrolyte carriers since electron-hole separation happens in TiO₂/CdSe

interface as results, electrons are conducted to FTO layer through TiO₂ film and holes remain on CdSe nanospherical particles. Therefore, as electron and hole are situated in two different compounds, the recombination rate is reduced consequently [14, 18].

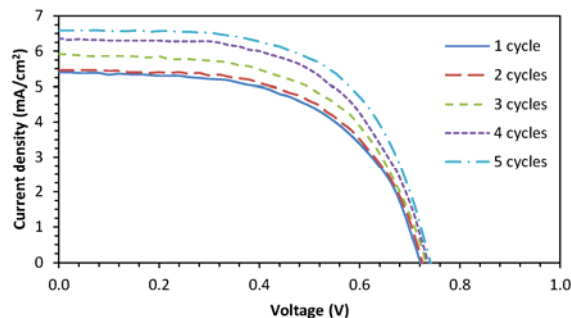


Fig. 5. Photocurrent density-voltage curves of the DSSCs made of CdSe nanospherical particles sensitized mesoporous TiO₂ films after different SILAR cycles.

Table 1. Photovoltaic parameters of the DSSCs made of CdSe nanospherical particles sensitized mesoporous TiO₂ films after different SILAR cycles.

SILAR cycles	J _{SC} (mA/cm ²)	V _{OC} (V)	FF	η (%)
1	5.40	0.721	0.57	2.22
2	5.46	0.726	0.59	2.34
3	5.92	0.732	0.58	2.51
4	6.36	0.736	0.59	2.76
5	6.59	0.742	0.60	2.93

4. Conclusions

The mesoporous TiO₂ films used as the photoanodes of the DSSCs with the aim of a better incident light harvesting were sensitized by CdSe nanospherical particles with a simple and low-cost method, SILAR. SEM images showed that CdSe individual nanoparticles were formed on the surface of mesoporous TiO₂ films with novel spherical shape, and with the enhancement of SILAR cycles, their amount increased so much that after five SILAR cycles, they joined and formed a porous cover on the surface of mesoporous TiO₂ film. The three dimensional AFM pictures of the surface of samples illustrated that they all had approximately a uniform hill-valley like morphology. The comparison of the absorbance spectra demonstrated that with the enhancement of SILAR cycles, the absorption increased and the absorption edges shifted to the longer wavelengths. Photovoltaic measurements clarified that the short circuit current and the open circuit voltage were increased with the enhancement of SILAR cycles and reached to 6.59 mA/cm² and 0.742 V after five SILAR cycles, respectively. As a result, the solar cells sensitized by CdSe

nanospherical particles had the minimum power conversion efficiency of 2.22 % after one SILAR cycle and obtained the maximum power conversion efficiency of 2.93 % after five SILAR cycles.

References

- [1] M. Gratzel, *Inorganic Chemistry* **44**, 6841 (2005).
- [2] B. O'Regan, M. Gratzel, *Nature* **353**, 737 (1991).
- [3] S.L. Chung, C.M. Wang, *Journal of Materials Science and Technology* **28**, 713 (2012).
- [4] Y. Fu, Z. Jin, Y. Ni, H. Du, T. Wang, *Thin Solid Films* **517**, 5634 (2009).
- [5] J.M. Szeifert, D. Fattakhova-Rohlfing, D. Georgiadou, V. Kalousek, J. Rathousky, D. Kuang, S. Wenger, S.M. Zakeeraddin, M. Gratzel, T. Bein, *Chemistry of Materials* **21**, 1260 (2009).
- [6] S. Ngamsinlapasathian, S. Pavasupree, Y. Suzuki, S. Yoshikawa, *Solar Energy Materials & Solar Cells* **90**, 3187 (2006).
- [7] P. Sudhagar, J.H. Jung, S. Park, R. Sathyamoorthy, H. Ahn, Y.S. Kang, *Electrochimica Acta* **55**, 113 (2009).
- [8] K. Prabakar, H. Seo, M. Son, H. Kim, *Materials Chemistry and Physics* **117**, 26 (2009).
- [9] H. Chen, W. Li, H. Liu, L. Zhu, *Solar Energy* **84**, 1201 (2010).
- [10] W. Lee, S.K. Min, V. Dhas, S.B. Ogale, S.H. Han, *Electrochemistry Communications* **11**, 103 (2009).
- [11] S.Q. Fan, D. Kim, J.J. Kim, D.W. Jung, S.O. Kang, J. Ko, *Electrochemistry Communications* **11**, 1337 (2009).
- [12] Q. Shen, M. Yanai, K. Katayama, T. Sawada, T. Toyoda, *Chemical Physics Letters* **442**, 89 (2007).
- [13] M.A. Hernandez-Pereza, J. Aguilar-Hernandez, G. Contreras-Puente, J.R. Vargas-Garcia, E. Rangel-Salinas, *Physica E* **40**, 2535 (2008).
- [14] W. Lee, W.C. Kwak, S.K. Min, J.C. Lee, W.S. Chae, Y.M. Sung, S.H. Han, *Electrochemistry Communications* **10**, 1699 (2008).
- [15] Y. Zhang, J. Zhu, X. Yu, J. Wei, L. Hu, S. Dai, *Solar Energy* **86**, 964 (2012).
- [16] L.W. Chong, H.T. Chien, Y.L. Lee, *Journal of Power Sources* **195**, 5109 (2010).
- [17] S.B. Rawal, S.D. Sung, S.Y. Moon, Y.J. Shin, W.I. Lee, *Materials Letters* **82**, 240 (2012).
- [18] J. Deng, M. Wang, X. Song, Y. Shi, X. Zhang, *Journal of Colloid and Interface Science* **388**, 118 (2012).

*Corresponding author: byarmand@merc.ac.ir